

# III-V/SOI heterogeneous photonic integrated devices for optical interconnection in LSI

著者	Nishiyama Nobuhiko, Maruyama Takeo, Ara Shigehisa
journal or publication title	Conference Proceedings - International Conference on Indium Phosphide and Related Materials
volume	5012485
page range	210-214
year	2009-01-01
URL	<a href="http://hdl.handle.net/2297/20303">http://hdl.handle.net/2297/20303</a>

doi: 10.1109/ICIPRM.2009.5012485

## III-V/SOI heterogeneous photonic integrated devices for optical interconnection in LSI

Nobuhiko NISHIYAMA<sup>1</sup>, Takeo MARUYAMA<sup>3</sup>, and Shigehisa ARAI<sup>1,2</sup>

<sup>1</sup> Department of Electrical and Electronic Engineering, <sup>2</sup>Quantum Nanoelectronics Research Center  
Tokyo Institute of Technology

2-12-1-S3-12 O-okayama, Meguro-ku, Tokyo 152-8552, Japan

<sup>3</sup> School of Electrical and Computer Engineering, Kanazawa University  
n-nishi@pe.titech.ac.jp

**Abstract**—InP-based photonic devices on SOI substrate using bonding technologies were demonstrated. Direct bonding and BCB bonding enable us to realize high optical confinement DFB lasers and other devices for intra/inter-chip connection in Si LSI circuit. Low threshold optical pumped membrane lasers and CW-operation of lateral current injection lasers with thin lateral cladding lasers were realized.

*Keywords* Silicon On Insulator, III-V semiconductor, Wafer Bonding Photonic Integrated Circuit.

### I. INTRODUCTION

Photonic devices have given a solution for long-distance and high speed communication. Two major components in this photonic network are optical fibers and semiconductor lasers, which are made by combinations of III-V semiconductors such as InP- or GaAs-based materials. III-V semiconductors have variety of combinations to generate wide optical wavelength range from visible to infrared. More importantly, they can have direct bandgap properties to generate photons efficiently compared with indirect bandgap materials such as Si and Ge. Several proposals to increase emission efficiency of Si-based materials such as utilizing quantum effect of nanostructure [1] and impurity doping [2] have been proposed. So far, enough optical gain from these structures to achieve lasing operation has not been demonstrated. Therefore, using III-V materials are dominant way for optical devices.

On the other hand, Si is a major semiconductor material for electrical LSI circuits due to its simple material properties. The speed of the LSI is getting higher and higher by the reduction of device sizes. However, the speed and the power consumption are reaching their limits due to transmission time delay caused by long total global transmission line distance [3]. To solve this problem, many researchers proposed to use optical circuits and demonstrated optical devices using Si or silicon-on-insulator (SOI) substrates [4-6]. In addition to this, introducing III-V materials is crucial to realize high performance active optical (photonic) devices such as lasers and amplifiers because of the advantages mentioned above. Growing III-V materials directly on Si substrates was tried by many researchers for a long time and several interesting results were reported [7,8]. However, the growth could not be done on amorphous Si or SiO<sub>2</sub>, which is the surface of Si LSI circuits.

Therefore, to integrate III-V devices on Si, so-called heterogeneous integration, wafer bonding technology is a practical solution at this moment. In this paper, integration technologies and device performance will be reviewed.

### II. WAFER BONDING

To bond Si and III-V wafers, two methods are carried out, a direct bonding method [9, 10] and a benzocyclobutene (BCB) bonding method [11]. The direct bonding is the method to bond two wafers without any glue. Plasma activated surfaces by N<sub>2</sub> or hydrophilic surfaces were used. Figure 1 shows the bonding strength of two independent Si wafers after the surface activation and pressurization under 250 °C as a function of applied pressure. The bonding strength of >1 MPa can be achieved. Figure 2 (a) shows a SEM image of the bonding interface between SOI and InP laser wafers after removing host InP substrate. No air void can be observed. For some device configurations, alignment between two wafers is required. An infrared (IR) camera *in-situ* monitor system and motorized stages are installed in our high vacuum bonding chamber. Figure 2(b) shows IR camera image after bonding using *in-situ* alignment. The accuracy of the alignment is less than 3 μm. By introducing this alignment technology, InP and Si wafers can be fabricated separately and bonded at a late process. This is important since some process parameters such as maximum temperature and choice of metal materials are different between Si LSI and III-V processes.

For wafers which have bumpy surfaces, a wafer bonding process by BCB is suitable. The keys to make a smooth bonding interface are bonding under low chamber pressure and controlling the viscosity of precursor to avoid air voids [12].

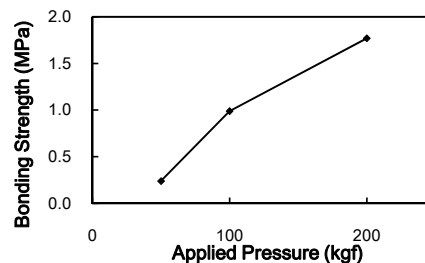
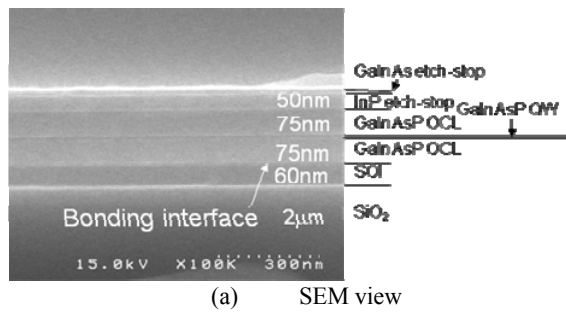
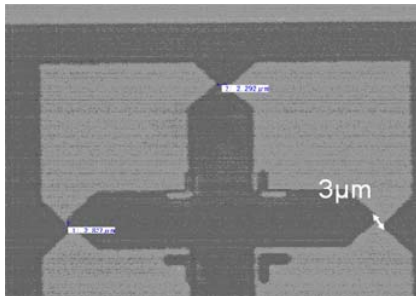


Fig.1 Bonding strength after plasma activated bonding under 250 °C as a function of applied pressure.



(a) SEM view



(b) Top IR image. A center cross and an outside anchor mark are on a top wafer and a bottom wafer, respectively.

Fig.2 Pictures of bonded wafers

### III. LASER PERFORMANCE

Using the direct bonding technology, GaInAsP/InP DFB lasers on an SOI substrate with wire-like active regions have been demonstrated [13]. The fabricated device structure is shown in Fig. 3. An InP wafer consists of double quantum wells (QWs) sandwiched by GaInAsP optical confinement layers (OCLs) on an InP host substrate grown by low pressure metal organic chemical vapor deposition (MOCVD). QWs were partially etched by electron beam lithography and dry etching and the etched trenches were filled by InP layer by regrowth to form a feedback grating. The active mesa width and the grating period are 120 nm and 242.5 nm, respectively. The SOI wafer consists of a 200 nm Si layer and a 2 μm SiO<sub>2</sub> layer on a Si substrate. After bonding, the InP host substrate was wet etched followed by formation of 25-μm-wide stripes and metal contacts.

Figure 4 shows the spectrum under 0.1 % duty pulsed condition at room temperature. A side-mode suppression ratio (SMSR) of 28 dB at 1.3 times threshold current has been achieved. The threshold current was as high as 104 mA at this moment due to the wide stripe width. Although the device structure had the high index Si layer below the III-V layer, the optical confinement factor of the active layers was comparable to that of conventional InP-based lasers.

To reduce the threshold current beyond conventional edge emitting lasers, a membrane structure with only a 150-nm thick III-V core layer has been proposed. The membrane structure consists of the III-V core layer sandwiched by low index materials such as SiO<sub>2</sub> and BCB as cladding layers. Due to this large index difference, this structure gives us ~3 times higher optical confinement factor than that of conventional edge emitting lasers which have semiconductor cladding layers as shown in Fig. 5. By combination of this high optical confinement factor and strong grating coupling structures such as the wire-like

active regions mentioned above and surface corrugation gratings, threshold can be further reduced. So far, lasing operation of a membrane laser with the surface corrugation grating under optical pumping has been demonstrated as shown in Fig. 6 [14]. The wavelength of the pumping light was 980 nm. Only 0.34 mW pumping power was needed to reach threshold for lasing. If the absorption coefficient of pumping light in the membrane laser was assumed to be 10000 cm<sup>-1</sup>, the corresponding threshold current was estimated to be 24 μA. Experimental and calculated lasing spectra are shown in Fig. 7. A stable single-mode operation with an SMSR of 35 dB was obtained at the bias of 2 times threshold power. Since this laser had the surface corrugation grating with high index difference, the coupling coefficient was estimated to be 4200 cm<sup>-1</sup>, which was quite larger than that of conventional DFB lasers.

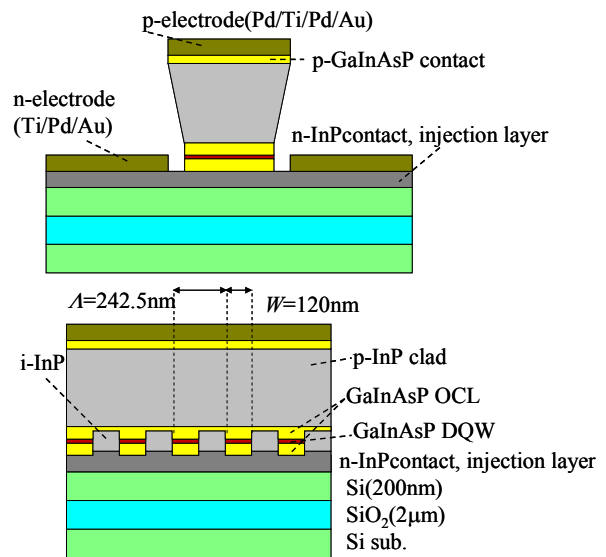


Fig. 3 The schematic diagram of DFB lasers on SOI.

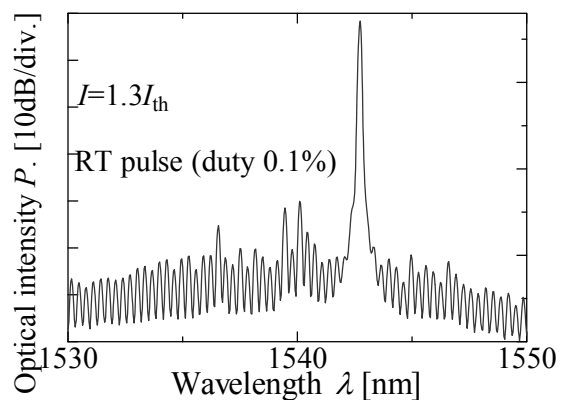
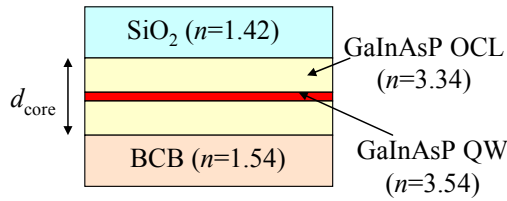


Fig. 4 Spectrum of the fabricated DFB laser.

(a) Membrane Structure



(b) Conventional Structure

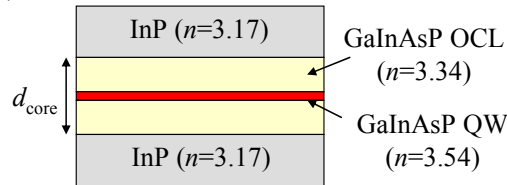


Fig. 5 Schematic diagrams of semiconductor lasers.

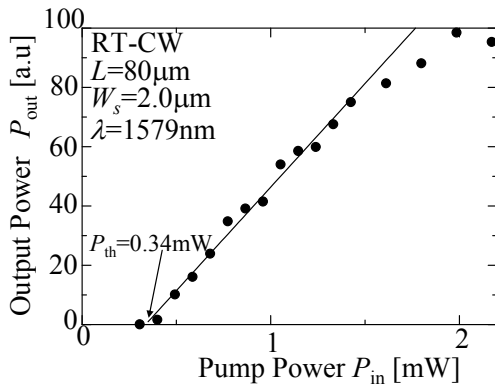


Fig. 6 Lasing characteristics of an optical pumped GaInAsP membrane laser.

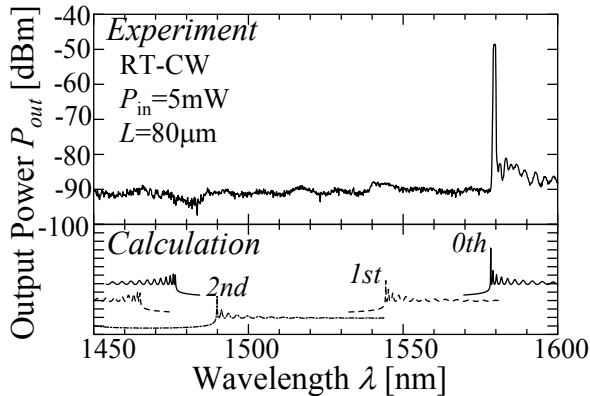


Fig. 7 Measured and calculated lasing spectra of the membrane laser. The dotted line spectra in the calculation results are spectra for higher order transverse modes.

The membrane structure also has an advantage in terms of coupling efficiency from lasers to Si wire passive waveguides. Figure 8 shows the calculation results of the coupling efficiency

to a Si wire waveguide from a Si waveguide integrated membrane laser and this threshold current density as a function of upper Si layer thickness in a SOI substrate. The Si layer thickness of conventional SOI wafers for optical waveguide is about 200 nm. Therefore, >80% coupling efficiency and <100 A/cm<sup>2</sup> can be expected. As the Si layer thickness increases, the coupling efficiency increases, however, the threshold current of the lasers also increases due to less optical confinement in the active regions of the lasers.

In this moment, the lasing operation of an optical pumped SOI integrated membrane laser has been demonstrated [9]. The biggest problem of this membrane structure is that a vertical current injection structure, which is used in most of edge emitting lasers, cannot be used since the cladding layer materials are insulators. Therefore, a lateral current injection structure is needed to be introduced. Recently, continuous wave (CW) lasing operation of lateral current injection lasers with 400-nm-thick lateral cladding layers on semi-insulated (SI) substrate was achieved to emulate the membrane laser structures [15]. The structure consists of GaInAsP QWs with 150-nm-thick OCLs sandwiched by p-InP and n-InP cladding layers laterally using photolithography and double regrowth technique. Figure 9 shows I-L-V characteristics under CW condition at room temperature. The threshold current is 12 mA for 490 μm cavity length and 1.4 μm stripe width. Although the external differential quantum efficiency was as low as 12.5% due to current leakage and the electrical resistance was as high as 37 Ω, this can be fixed by modifying the materials in the center active region and doping profile according to our calculation.

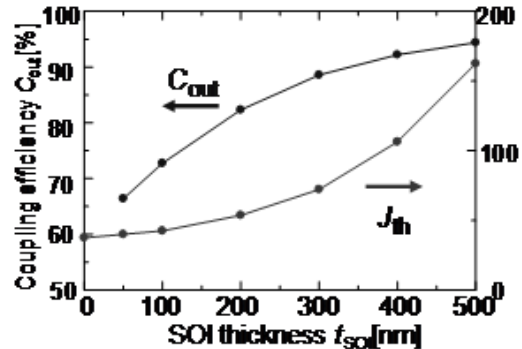


Fig. 8 Calculated coupling efficiency to an integrated Si wire waveguide and threshold current density of membrane lasers on SOI.

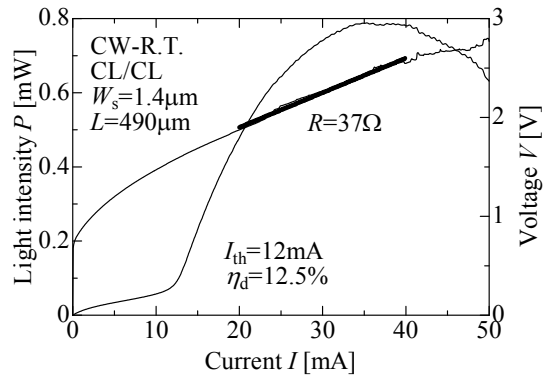


Fig. 9 I-L-V characteristics of the fabricated lateral current injection laser.

#### IV. OTHER DEVICES

The wafer bonding technology can be applicable for other photonic devices such as semiconductor optical amplifiers [16] and modulators [17]. In addition to this, high index contrast III-V wire waveguides can be realized on Si using BCB bonding as shown in Fig. 10 [12]. GaInAsP wire waveguides with  $150 \times 500 \text{ nm}^2$  core surrounded by BCB and  $\text{SiO}_2$  cladding on Si substrate were achieved. The propagation loss was 2.1 dB/mm, which is 10 times higher than that of Si wire waveguide, however, lower than that of other III-V wire waveguides previously reported. Since the waveguides have large optical index difference, bending loss can be small even at tight bending radius. Similar optical bending loss compared with Si-wire waveguides on SOI can be achieved. Figure 11 shows the bending loss per 90 degree bend as a function of bending radius. Less than 1 dB loss was achieved for larger than  $1.5 \mu\text{m}$  bending radius. This waveguide could be used for not only passive waveguide to connect devices, but also other function. By choosing proper materials and waveguide structures, very high nonlinear effect can be expected due to high optical confinement for wavelength conversion.

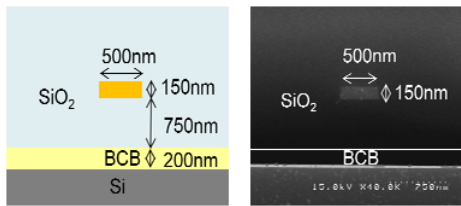


Fig. 10 An SEM image of GaInAsP wired waveguide on Si.

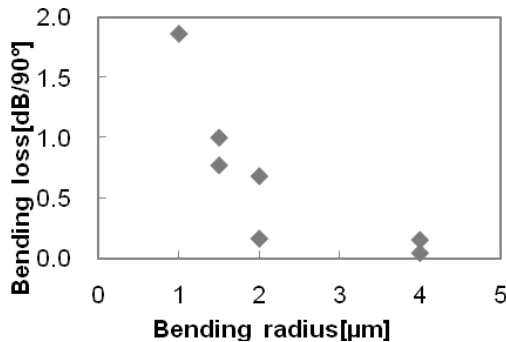


Fig.11 Bending loss of the fabricated GaInAsP wired waveguide as a function of bending radius.

#### V. CONCLUSION

Heterogeneous integration technologies using wafer bonding techniques are reviewed. These technologies allow us to realize high performance photonic devices on Si and can be integrated with electrical LSI circuits.

#### ACKNOWLEDGMENT

The authors would like to thank our students and Mr. S. Tamura to produce the results in this paper. We also would like to thank Prof. K. Furuya, Prof. M. Asada, Prof. T. Mizumoto, Prof. Y. Miyamoto and Prof. M. Watanabe for helping the project. This research was supported by a Grant-in-Aid for Scientific Research (#19002009, #19686023, #19760231) from the Ministry of Education, Culture, Sports, Science and Technology (MEXT)

#### REFERENCES

- [1] S. Saito, D. Hisamoto, H. Shimizu, H. Hamamura, R. Tsuchiya, Y. Matsui, T. Mine, T. Arai, N. Sugii, K. Torii, S. Kimura, and T. Onai, "Silicon light-emitting transistor for on-chip optical interconnection," *Appl. Phys. Lett.*, Vol. 89, No. 16, pp. 163504-1-3, Oct. 2006.
- [2] W. L. Ng, M. A. Lourenco, R. M. Gwilliam, S. Ledain, G. Shao, and K. P. Homewood, "An efficient room-temperature silicon-based light-emitting diode," *Nature*, Vol. 410, No. 6825, pp. 192-194, Mar. 2001.
- [3] D. A. B. Miller, "Rationale and challenges for optical interconnects to electronic chips," *Proc. IEEE*, Vol. 88, No. 6, pp. 728-749, Jun. 2000.
- [4] J. Foresi, P. Villeneuve, J. Ferrara, E. Thoen, G. Steinmeyer, S. Fan, J. Joannopoulos, L. Kimerling, H. Smith, and E. Ippen, "Photonic bandgap microcavities in optical waveguides," *Nature*, Vol. 390, No. 13, pp. 143-147, Nov. 1997.
- [5] A. Sakai, G. Hara, and T. Baba, "Propagation Characteristics of Ultrahigh- $\Delta$  Optical Waveguide on Silicon-on-Insulator Substrate," *Jpn. J. Appl. Phys.*, Vol. 40, No. 4B, pp. L383-L385, Apr. 2001.
- [6] A. S. Liu, R. Jones, L. Liao, D. Samara-Rubio, D. Rubin, O. Cohen, R. Nicolaescu, and M. Paniccia, "A high speed silicon optical modulator based on a metal-oxide-semiconductor capacitor," *Nature* Vol. 427, No. 7, pp. 615-618, Feb. 2004.
- [7] K. K. Linder, J. Phillips, O. Qasaimeh, X. F. Liu, S. Krishna, P. Bhattacharya, and J. C. Jiang, "Self-organized  $\text{In}_{0.4}\text{Ga}_{0.6}\text{As}$  quantum-dot lasers grown on Si substrates," *Appl. Phys. Lett.*, Vol. 74, No.10, pp.1355-1357, Mar. 1999.
- [8] A. Jallipalli, M. N. Kutty, G. Balakrishnan, J. Tatebayashi, N. Nuntawong, S. H. Huang, L. R. Dawson, D. L. Huffaker, Z. Mi, and P. Bhattacharya, "1.54  $\mu\text{m}$  GaSb/AlGaSb multi-quantum-well monolithic laser at 77 K grown on miscut Si substrate using interfacial misfit arrays," *Electron. Lett.*, Vol. 43, No. 22., Oct. 2007.
- [9] T. Maruyama, T. Okumura, S. Sakamoto, K. Miura, Y. Nishimoto, and S. Arai, "GaInAsP/InP membrane BH-DFB lasers directly bonded on SOI substrate," *Optics Express*, Vol. 14, No. 18, pp. 8184-8188, Sept. 2006.
- [10] A. W. Fang, H. Park, O. Cohen, R. Jones, M. Paniccia, and J. E. Bowers, "Electrically pumped hybrid AlGaInAs-silicon evanescent laser," *Optics Express*, Vol. 14, No. 20, pp. 9203-9210, Oct. 2006.
- [11] G. Roelkens, D. Van Thourhout, R. Baets, R. Notzel, and M. Smit, "Laser emission and photodetection in an InP/InGaAsP layer integrated on and coupled to a Silicon-on-Insulator waveguide circuit," *Optics Express*, Vol. 14, No. 18, pp. 8154-8159, Sept. 2006.

- [12] H. Enomoto, K. Inoue, T. Okumura, H. D. Nguyen, N. Nishiyama, Y. Atsumi, S. Kondo, and S. Arai, "Properties of high index contrast wired GaInAsP waveguides with benzocyclobutene on Si substrate" *Digest of IPRM 2009*, ThA1.4, Newport Beach, CA, May 2009.
- [13] T. Okumura, T. Maruyama, H. Yonezawa, N. Nishiyama, and S. Arai, "Injection-Type GaInAsP-InP-Si Distributed-Feedback Laser Directly Bonded on Silicon-on-Insulator Substrate," *Photon. Tech. Lett.*, Vol. 21, No. 5, pp. 283-285, Mar. 2009.
- [14] S. Sakamoto, H. Naitoh, T. Ohtake, Y. Nishimoto, T. Maruyama, N. Nishiyama, and S. Arai, "85 °C Continuous-Wave Operation of GaInAsP/InP-Membrane Buried Heterostructure Distributed Feedback Lasers with Polymer Cladding Layer" *Jpn. J. Appl. Phys.*, Vol. 46, No. 47, pp. L1155-L1157, Nov. 2007.
- [15] T. Okumura, M. Kurokawa, D. Kondo, H. Ito, N. Nishiyama, and S. Arai, "Lateral Current Injection Type GaInAsP/InP DFB Lasers on SI-InP Substrate," *Digest of IPRM 2009*, TuB2.5, Newport Beach, CA, May 2009.
- [16] H. Park, Y.-h. Kuo, A. W. Fang, R. Jones, O. Cohen, M. J. Paniccia, and J. E. Bowers, "A hybrid AlGaInAs-silicon evanescent preamplifier and photodetector," *Opt. Express*, Vol. 15, No. 21, pp. 13539-pp. 13546, Oct. 2007.
- [17] Y. -H. Kuo, H. -W. Chen, and J. E. Bowers, "High speed hybrid silicon evanescent electroabsorption modulator," *Optics Express* , Vol. 16, No. 13, pp. 9936-9941, Jun. 2008.